Angewandte Chemie
Eine Zeitschrift der Gesellschaft Deutscher Chemiker

Supporting Information

Long-Lasting Efficacy of Coatings for Bronze Artwork Conservation: The Key Role of Layered Double Hydroxide Nanocarriers in Protecting Corrosion Inhibitors from Photodegradation

Martina Salzano de Luna, Giovanna G. Buonocore, Chiara Giuliani, Elena Messina, Gabriella Di Carlo, Marino Lavorgna, Luigi Ambrosio, and Gabriel M. Ingo*

anie_201713234_sm_miscellaneous_information.pdf

Supporting Information

Table of Contents

S1. Experimental Procedures

S1.1. Materials

Highly amorphous polyvinyl alcohol (HAVOH, G-Polymer grade OKS-8049) was purchased from Nippon Synthetic Chemical Industry Co., Ltd., Japan. Poly(allylamine) (PAA, average molecular weight 17 kDa) was purchased from Sigma Aldrich, Italy. The 2-mercaptobenzothiazole (MBT, purity 98%) powder was purchased from Sigma Aldrich (Italy).

Zn-Al layered double hydroxide nanocarriers loaded with MBT molecules (LDH/MBT) by anion-exchange reaction were produced by Prolabin & Tefarm s.r.l. (Italy). The presence of intercalated MBT can be clearly appreciated by FTIR analysis. The FTIR spectra of MBT and LDH/MBT powders are shown in Figure S1a. In the spectrum of the MBT loaded nanocarriers, the presence of the inhibitor molecules can be recognized from the MBT characteristic bands at ~3000 cm^{-1} (C-H deformation), ~1360 cm^{-1} (C=N stretching), and ~1010 cm^{-1} (C-C-C bending). In addition, the variation of the position of the

peaks with respect to pristine MBT powder is indicative of the interaction between the intercalated anions and the positively charged hydroxide layers. The presence of MBT ions intercalated in the brucite-like layer of LDH nanocarriers is also confirmed by X-ray diffraction (XRD) analysis (Figure S1b). Indeed, the XRD spectrum of LDH/MBT nanocarriers is characterized by asymmetric and broad peaks (see for example inset of Figure S1b) revealing the existence of two LDH-type phases, which in turn reflect the presence of guest anions in two different orientations within the interlayer galleries, as already found in LDH nanoparticles intercalated with big organic molecules.[1] The basal spacing *d*(003) associated with these two phases was estimated to be ~1.72 nm (phase #1) and ~0.80 nm (phase #2), in good agreement with the results reported by Ferreira and co-workers for Zn-Al LDH loaded with MBT molecules.[1a, 1b] The amount of MBT in the LDH nanocarriers was determined by complete dissolution of the inorganic nanoparticles in a 0.1 M HNO_3 solution, followed by UV-Vis measurement of the resulting MBT in solution.[2] The MBT loading in the LDH nanocarriers was estimated to be 36 ± 1 wt%.
Finally, a bronze alloy was used as metal substrate (Cu: 85 wt%, Sn: 5 wt%, Pb: 5 wt%, Zn: 5 wt %).

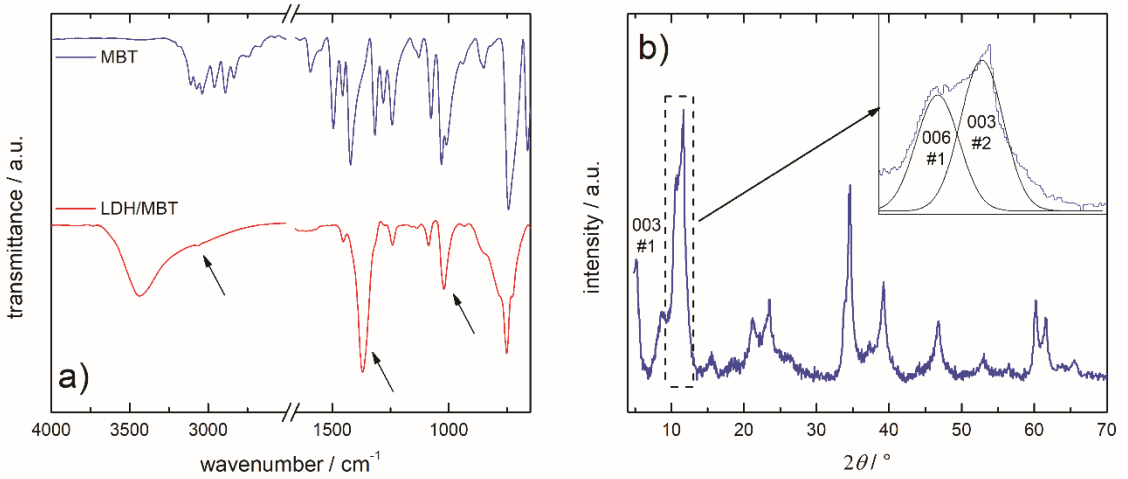

Figure S1. a) FTIR and b) XRD spectra of MBT and LDH/MBT powders. FTIR spectra in a) were vertically shifted for the sake of clarity.

S1.2. Preparation of HAVOH-Based Formulations and Coatings

The coating formulations were prepared by dissolving HAVOH (5 wt/vol%) in a mixture of bi-distilled water and ethanol (50/50 vol/vol%) by magnetic stirring at room temperature for about 3 hours. The composition of the water/ethanol mixture was selected as tradeoff between wettability on bronze disks and polymer solubility. Then, the PAA solution was added dropwise to the HAVOH one (PAA/HAVOH weight ratio of 0.1). The amount of PAA was selected as the minimum content that allows the realization of transparent and homogenous coatings. LDH nanocarriers were dispersed in water/ethanol (1.5 g L^{-1}) by sonication for 15 minutes, and MBT powder was dissolved in water/ethanol (0.5 g L^{-1}) by magnetic stirring at room temperature. For the formulation with the nanocarriers (HAVOH-LDH/MBT coatings), a proper volume of LDH dispersion was added to the HAVOH/PAA solution.
The amount of nanocarriers within the coating was selected in the light of preliminary analyses in order to maximize the amount of corrosion inhibitor yet preserving the coating transparency. For this purpose, HAVOH-LDH coatings with different LDH content and coating thickness were deposited on glass slides, and then their UV-Vis spectra were acquired in transmittance mode. The average transmittance, T_{av}, in the visible range of wavelengths (390-700 nm) is reported in Figure S2 as a function of the weight percentage of LDH nanocarriers with respect to the amount of polymeric phase, m_{LDH}, for coatings having different thickness. Note that the corresponding weight percentage of MBT with respect to the amount of polymeric phase, m_{MBT}, was also shown (top x-axis). The coatings in the red-shaded area were excluded because the amount of MBT introduced within the coatings by addition of LDH nanocarriers is too low; whereas those in the black-shaded area

were excluded due to the low transparency, which is not appropriate for possible application in cultural heritage conservation. According to the data shown in Figure S2, m_{LDH} = 5.5 wt% was selected for the HAVOH-LDH/MBT coatings, as it ensures a sufficiently high amount of MBT (≈2 wt%) and almost negligible loss of coating transparency (T_{av} > 97%). Accordingly, for the formulation with the freely dispersed corrosion inhibitor (HAVOH-MBT coatings), the MBT solution was added to the HAVOH/PAA one to get the same amount of MBT with respect to the amount of polymeric phase (i.e. m_{MBT} = 2 wt%). Before coating deposition, the bronze disks (diameter: ~30 mm, thickness: ~5 mm) were polished by using SiC papers at 1200 and 2500 grit, and then with diamond pastes up to 3 µm to obtain a flat and smooth surface with a mirror-like finishing. After polishing, the Cu-based alloys have been cleaned with ethanol. Finally, the coatings were obtained by drop-casting the HAVOH-based solution on the bronze disks. For UV-Vis spectroscopy analyses, the coatings were deposited on fused quartz glass slides by the aid of a PDMS mask (see Section S2.3 for details). Glass slides were previously cleaned by a 3-step sonication process in acetone, isopropyl alcohol and bi-distilled water baths, followed by blow-drying with nitrogen gas.

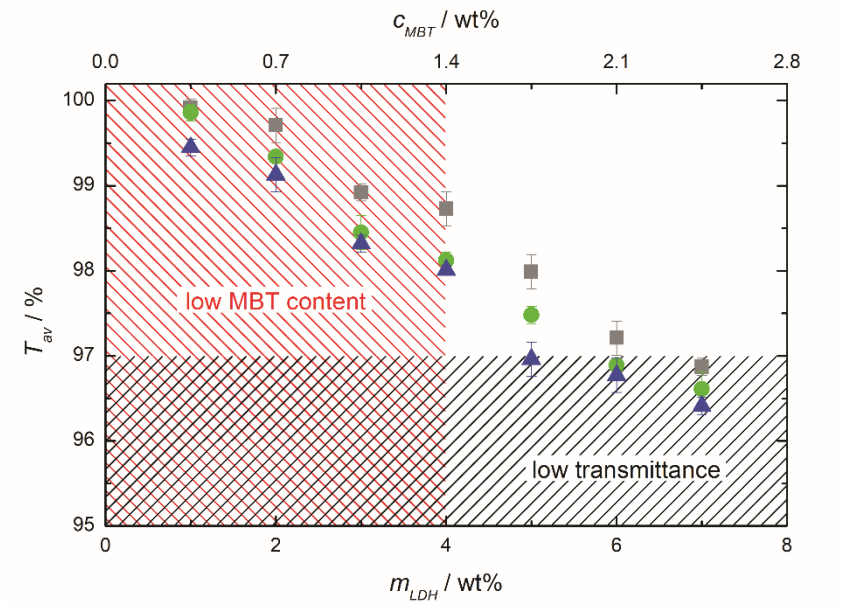

Figure S2. Average transmittance as a function of the weight percentage of LDH nanocarriers for HAVOH-LDH/MBT coatings having different thickness: 2 (squares), 4 (circles), 6 (triangles) µm. In the top x-axis, the corresponding weight percentage of MBT is also reported.

S1.3. Preparation of HAVOH-Based Formulations Containing Commercial UV Absorbers

The ability of LDH nanocarriers of preserving MBT molecules from photodegradation was compared to that of commercially available reference products:

- Tinuvin® 5333-DW, which is an aqueous dispersion of a blend of UV absorbers and a hindered amine light stabilizer.
- Tinuvin® 477-DW, which is an aqueous UV absorber dispersion, in combination with Tinuvin® 123-DW, which is a solvent-free hindered amine light stabilizer.

According to the product datasheets, the amount of product to be added to the coating formulation depends on the dry-film thickness and on desired protection level. Due to the very low thickness of the investigated HAVOH-based coatings (~2 µm), relatively high concentrations of UV absorbers were needed in order to ensure the same protection efficacy achieved with LDH nanocarriers against MBT photodegradation. The tested formulations containing the commercial products consisted of:

- Formulation 1: HAVOH-MBT formulation (m_{MBT} = 2 wt%) with Tinuvin® 5333-DW.
- Formulation 2: HAVOH-MBT formulation (m_{MBT} = 2 wt%) a mixture of Tinuvin® 477 and of Tinuvin® 123.

S2. Methods

S2.1. Structural and Morphological Analyses

Scanning electron microscopy (SEM) analyses were carried out on LDH/MBT nanocarriers using a FEI Quanta 200 FEG microscope in high vacuum mode. The analyses were performed at 30 kV acceleration voltage. The powder was gently deposited on the holder and sputter coated with a 15 nm thick Au–Pd layer.

The coated bronze disks were investigated by optical microscopy (OM) before and after the accelerated corrosion treatments (see details in Section S2.4). In order to evaluate the protective efficacy of the coatings, modifications at the metal surface were analyzed by OM. The optical analysis was carried out by using a Leica MEF 4M microscope equipped with a digital camera (Leica DFC 280).

S2.2. UV and Artificial Light Irradiation Experiments

UV-induced photodegradation of MBT in HAVOH-based coatings was carried out in a home-made UV irradiation apparatus, which consisted in eight 15 W UV lamps (Actinic BL, Philips) emitting long-wave UV-A radiation in the 350-400 nm range installed on a bracket enclosed in an aerated aluminum box.[3] The coated glass slides were positioned at a distance of 20 cm from the lamps. The UV-Vis spectra of the coatings were recorded at different time intervals. UV irradiation was also performed on LDH dispersions in water/ethanol mixture (50/50 vol/vol%) to evaluate to evaluate the effect of UV exposure on MBT release in different media (water/ethanol, water/ethanol with NaCl 0.5 M, water/ethanol at pH ~4).

The real-time artificial light-induced photodegradation of MBT in in HAVOH-based coatings was investigated in an indoor environment. Specifically, coated glass slides were stored in a room without windows (3.5 m x 5 m ca.), which was illuminated only by artificial light (eight 26 W compact fluorescent lamps) for ~8 hours per day. Note that in the selected fluorescent lamps the UV radiation is almost completely absorbed by a phosphor coating on the inside of the glass tube. The UV-Vis spectra of the coatings were recorded at different time intervals. Note that the exposure time, t_{INDOOR}, refers to the total storage time and not only to the actual lighting time.

S2.3. UV-Vis Spectroscopy Analyses

The photodegradation of MBT in the HAVOH-based coatings was monitored by UV-Vis spectroscopy. The analyses were performed on HAVOH-MBT and HAVOH-LDH/MBT coatings deposited on glass slides. The analyses were performed on coatings with the same amount of MBT (m_{MBT} = 2 wt% with respect to the amount of polymeric phase, corresponding to m_{LDH} = 5.5 wt%) and thickness (2 µm). The UV-Vis spectra of the coatings were recorded by means of a Cary UV 60 UV-Vis spectrometer in the wavelength range of 250-800 nm. Fifteen different coatings were tested for each formulation. A bare glass slide was used for the baseline and neat HAVOH coatings were used as reference. Preliminary analyses were carried out to optimize the measurements. Specifically, rather than covering the whole glass slide, a tailor-made PDMS was used mask to obtain coatings with highly controlled thickness and having dimensions that fit those of the detector hole of the spectrophotometer. In addition, a custom-made support was used to fix the position of the glass slide during the tests. Figure S3 shows the UV-Vis spectra of three different HAVOH-MBT coatings deposited with the two different procedures. The perfect superposition of the spectra of coatings deposited with the PDMS mask (Figure S3b) confirms that the adopted expedients ensured the reliability and reproducibility of the measurements.

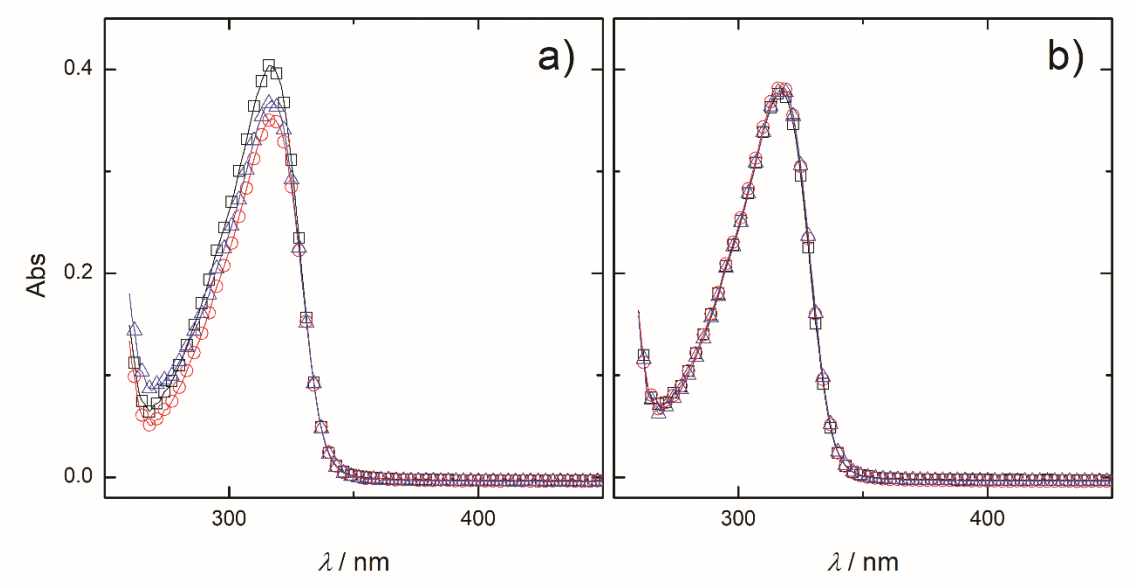

Figure S3. UV-Vis spectra of three representative HAVOH-MBT coatings deposited with different procedures: a) coating deposited on the entire glass slide, b) coating deposited by using the PDMS mask. All the coatings have at the same composition and thickness.

UV-Vis spectroscopy was also carried out on UV-treated LDH dispersions to evaluate the MBT release in different conditions. Finally, UV-Vis spectra were recorded also for UV-treated HAVOH-LDH/MBT coatings, which were then subjected also to the same process adopted for the accelerated corrosion treatment in order to verify the release of the MBT molecules form the nanocarriers into the coating.

S2.4. Accelerated Corrosion Treatments and Image Analysis Protocol

Accelerated corrosion treatment with acid vapors has been selected as more representative of indoor environments with respect to the commonly used electrochemical tests that are carried out by immersion in acidic solutions.[4] The advancement of corrosion processes is characterized by the formation of corrosion products, which are easily distinguishable from not corroded areas. Hence, image analysis was profitably exploited to characterize the state of the metal surface after accelerated corrosion tests of different duration. For this purpose, optical microscopy images at the metal/coating interface were collected without removing the coating, so as not to alter the state of the underlying metal surface. Then, a custom-tailored image analysis protocol was used to estimate the percentage corroded surface, S_{corr}, and thus to provide quantitative information about the protective efficacy of the HAVOH-based coatings. Before being analyzed, the images were pre-processed to adjust and equalize the basic tones. Then, they were converted from RGB images into grayscale ones. The threshold tone of the dark pixels associated with the corroded areas (due to the presence of corrosion products) was arbitrarily selected. Finally, the percentage of corroded area was estimated from the histograms corresponding to the relative frequency of the tones extracted from each grayscale image (we assigned a value of 0 to the white color and 100 to the black one, as limit values of the grayscale range). Images of untreated coated disk were used as reference. For each system, at least ten different optical micrographs were analyzed. An example of post-processed image is shown in Figure S4, together with the corresponding histogram of the relative frequency of the tones. For the sake of clarity, the color values of two representative sample points in the optical micrograph corresponding to not corroded (point 1) and corroded (point 2) areas are highlighted.

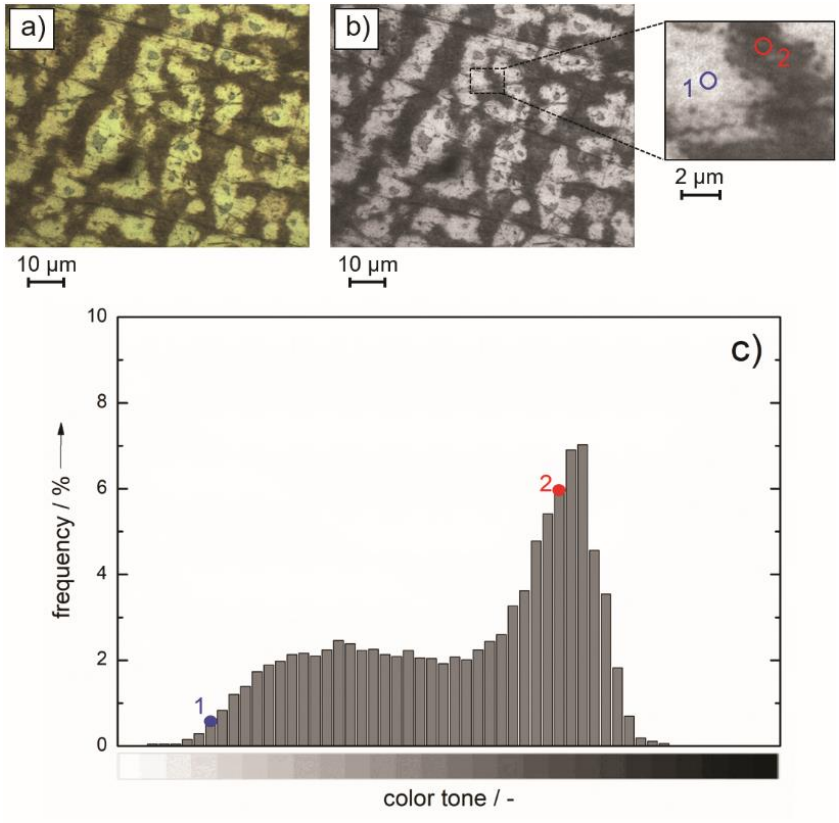

Figure S4. Representative optical micrograph of the disk surface at the metal/coating interface a) before and b) after processing and conversion into grayscale. c) Normalized distribution of the color tones of the grayscale image. The tones corresponding to the areas identified in the magnifications of the image are indicated in the histogram.

S2.5. ATR-FTIR Analyses

The pristine MBT powder and LDH nanocarriers were characterized by Attenuated Total Reflectance Fourier Transform Infrared (ATR-FTIR) spectroscopy. ATR-FTIR analyses were also carried out on HAVOH-MBT and HAVOH-LDH/MBT coatings. All the spectra were collected using a Perkin-Elmer FTIR Frontier spectrometer equipped with an ATR accessory. The measurements were recorded using a diamond crystal cell ATR at a resolution of 4 cm^{-1} and 32 scan collections. Baseline correction was applied to the reported spectra.

S3. Photodegradation of MBT in HAVOH-Based Coatings

S3.1. UV Exposure of Pristine HAVOH Coatings

Pristine HAVOH coatings were subjected to the same UV irradiation treatment carried out on HAVOH-MBT and HAVOH-LDH/MBT coatings and the UV-Vis spectra were reordered at different time intervals. The time evolution of the absorbance at 317 and 315 nm, which correspond to the λ^{peak} value of MBT in HAVOH-MBT and HAVOH-LDH/MBT coatings respectively, is shown in Figure S5. No significant variation of the absorbance values can be noticed, at least in the investigated timescale. Hence, the evolution of the normalized absorbance peak of MBT reported in the main text can be only ascribed to the photodegradation of the inhibitor molecules.

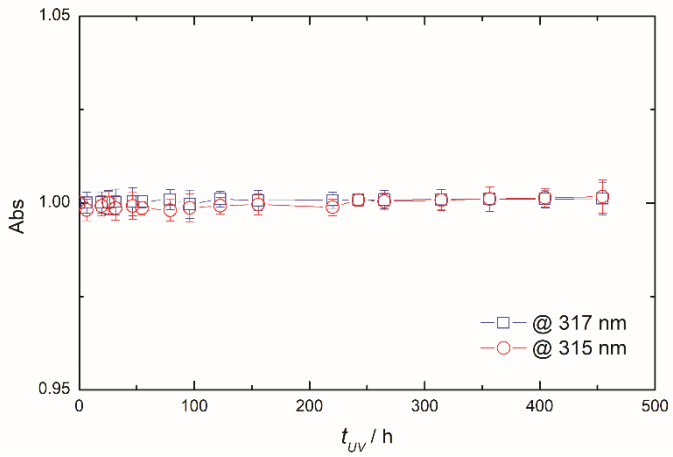

Figure S5. Time evolution of the absorbance at 317 (squares) and 315 (circles) nm of neat HAVOH coatings during UV exposure.

S3.2. MBT Stability in Dark Conditions

HAVOH-MBT and HAVOH-LDH/MBT coatings were stored under dark conditions to verify the stability of the corrosion inhibitor molecules in absence of artificial light or UV irradiation. The UV-Vis spectra of as-prepared coatings and coatings after 3 months storage under dark conditions are shown in Figure S6. Either when freely dispersed in the coating or loaded into LDH nanocarriers, the corrosion inhibitor molecules are stable, thus confirming that the effects reported in the main text are essentially due to the light-induced photodegradation of the MBT.

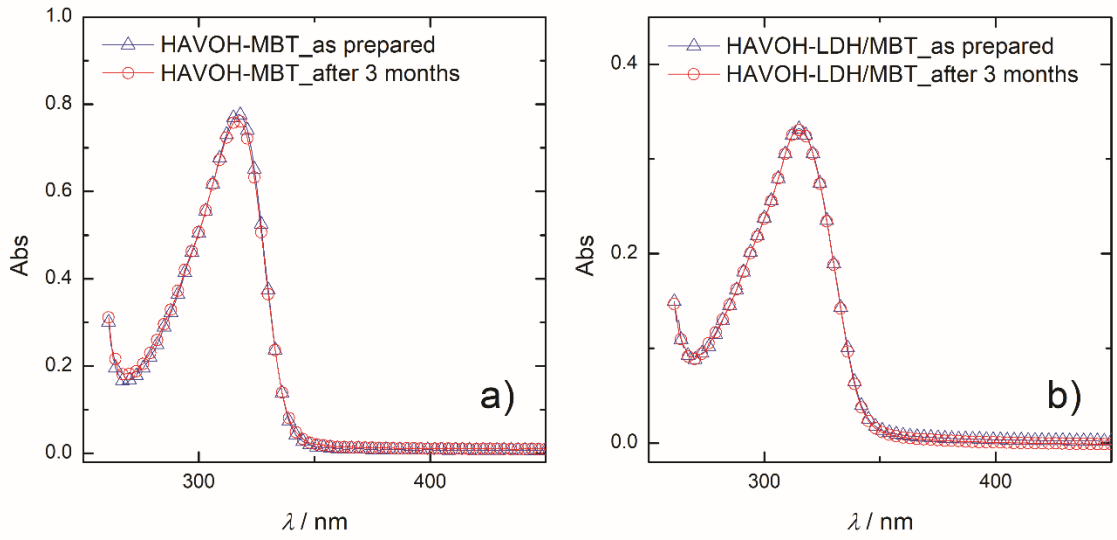

Figure S6. Representative UV-Vis spectra of a) HAVOH-MBT and b) HAVOH-LDH/MBT coatings: as-prepared coatings (red squares) and coatings stored for 3 months under dark conditions (blue circles). Not that the concentration of corrosion inhibitor is the same in the HAVOH+MBT and HAVOH+LDH/MBT coatings.

S3.3. ATR-FTIR Analysis of Coatings Before and After UV Exposure

ATR-FTIR analyses were exploited to verify the chemical stability of the coatings during UV irradiation. The spectra of the coatings before and after UV irradiation treatment of two weeks are shown in Figure S7. In all the investigated systems, the polymer matrix remains stable during UV exposure in the investigated time window. In particular, there is no appearance of new peaks and no significant shift of the characteristic vibrations of the as-prepared systems. We can thus exclude that the

MBT photodegradation and its consequent loss of anticorrosion efficacy can be related to possible interactions/reactions with other constituent of the coating or to other UV-induced changes in the polymer matrix.

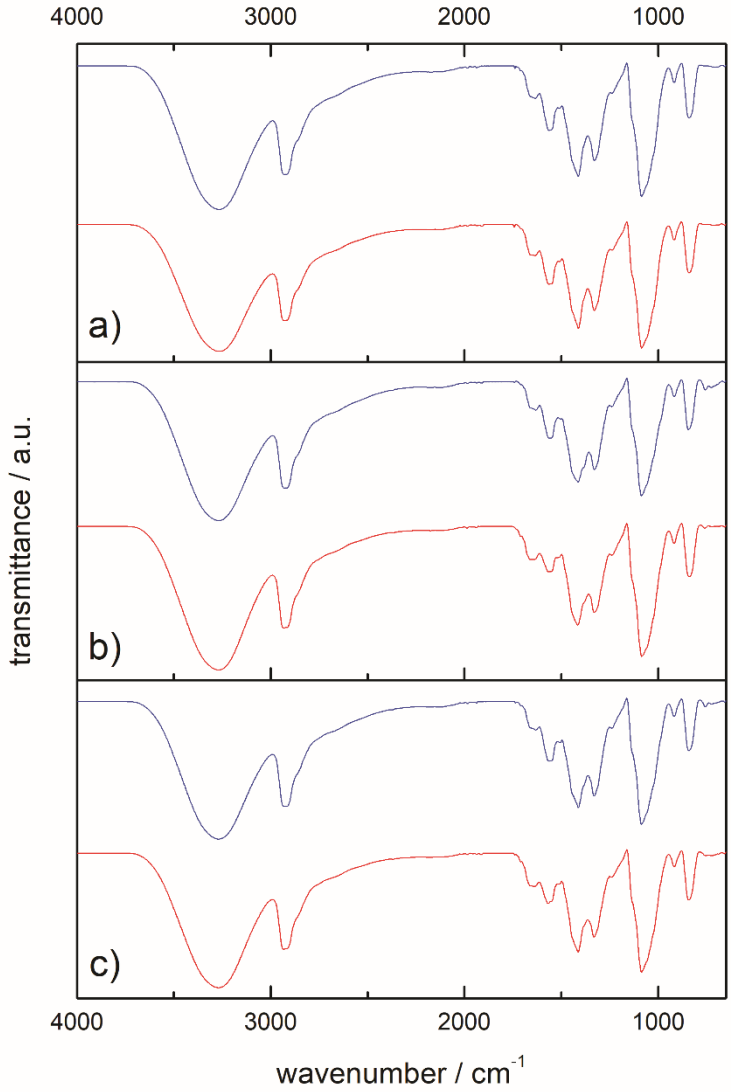

Figure S7. ATR-FTIR spectra of a) neat HAVOH, b) HAVOH-MBT and c) HAVOH-LDH/MBT coatings before (top curve) and after (bottom curve) two weeks of UV irradiation. Spectra were vertically shifted for the sake of clarity.

S3.4. Fitting of MBT Photodegradation Kinetics in HAVOH-Based Coatings

The time evolution of the normalized absorbance peak of MBT, A_N, during UV and artificial light irradiation treatments of the coatings (data shown in Figure 2a and 2b of the main text) has been fitted with different kinetic reaction models:[5]

First-order $A_N(t) = e^{-kt}$ (Eq. S1)

Second-order $A_N(t) = \frac{1}{1+kt}$ (Eq. S2)

Third-order $A_N(t) = \sqrt{\frac{1}{1+2kt}}$ (Eq. S3)

where $A_N(t)$ corresponds to the normalized absorbance peak of MBT at the generic time t, and k represents the rate constant of the process.

The results of the fitting procedure are shown in Figure S8 and the computed best fitting parameters are reported in Table S1.

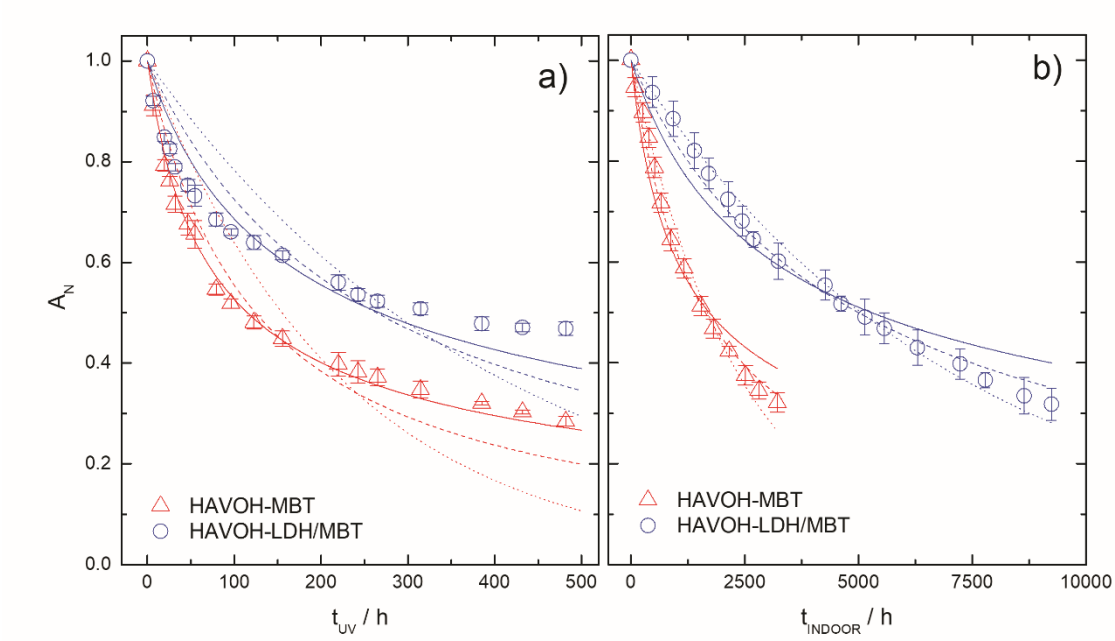

Figure S8. Experimental data of MBT photodegradation in HAVOH-MBT (triangles) and HAVOH-LDH/MBT (circles) coatings during a) UV exposure and b) artificial light irradiation (same data shown in figure 2a and 2b of the main text). Lines corresponds to the best fitting to first-order (dotted line), second-order (dashed line) and third-order (solid line) kinetic reaction models reported in Equations S1-S3, respectively.

Table S1. Parameters and regression coefficient obtained by fitting Equations S1-S3 to the experimental data of MBT photodegradation in the HAVOH-MBT and HAVOH-LDH/MBT coatings. The best fittings are in bold.

		UV exposure		*Artificial light exposure*	
System	Reaction kinetic model	k*10^3 [h^{-1}]	R^2	k*10^3 [h^{-1}]	R^2
HAVOH-MBT	First-order (Eq. S1)	4.47	0.7067	0.41	0.9836
	Second-order (Eq. S2)	8.03	0.9291	**0.61**	**0.9931**
	Third-order (Eq. S3)	**13.01**	**0.9946**	0.87	0.9581
HAVOH-LDH/MBT	First-order (Eq. S1)	2.44	0.5804	0.14	0.9877
	Second-order (Eq. S2)	3.79	0.7969	**0.20**	**0.9891**
	Third-order (Eq. S3)	**5.61**	**0.9196**	0.28	0.9451

References

[1] a) S. K. Poznyak, J. Tedim, L. M.Rodrigues, A. N. Salak, M. L. Zheludkevich, L. F. P. Dick, M. G. S. Ferreira, *ACS Appl. Mater. Interf.* **2009**, *1*, 2353-2362; b) J. Tedim, S. K. Poznyak, A. Kuznetsova, D. Raps, T. Hack, M. L. Zheludkevich, M. G. S. Ferreira, *ACS Appl. Mater. Interf.* **2010**, *2*, 1528-1535; c) T. Kameda, T. Yamazaki, T. Yoshioka, *Micropor. Mesopor. Mater.* **2008**, *114*, 410-415.

[2] J. Carneiro, A. F. Caetano, A. Kuznetsova, F. Maia, A. N. Salak, J. Tedim, N. Scharnagl, M. L. Zheludkevich, M. G. Ferreira, *RSC Adv.* **2015**, *5*, 39916-39929.

[3] Y. Zhu, G. G. Buonocore, M. Lavorgna, L. Ambrosio, *Polym. Compos.* **2011**, *32*, 519-528.

[4] F. Faraldi, B. Cortese, D. Caschera, G. Di Carlo, C. Riccucci, T. de Caro, G.M. Ingo, *Thin Solid Films* **2017**, *622*, 130-135.

[5] A. Khawam, D. R. Flanagan, *J. Phys. Chem. B* **2006**, *110*, 17315-17328.